The Spine Journal 19 (2019) 1106–1120

Basic Science

Effect of the type of electrical stimulation on spinal fusion in a rat posterolateral spinal fusion model

Pyung Goo Cho, MD[a], Gyu Yeol Ji, PhD[b], Yoon Ha, PhD[b], Hye Yeong Lee[c], Dong Ah Shin, MD, PhD[b,*]

[a] *Department of Neurosurgery, Bundang Jesaeng Hospital, Seongnam si, Republic of Korea*
[b] *Department of Neurosurgery, Yonsei University College of Medicine, Seoul, Republic of Korea*
[c] *Spine and Spinal Cord Institute, Department of Neurosurgery, Yonsei University College of Medicine, Seoul, Republic of Korea*

Received 30 September 2018; revised 19 December 2018; accepted 19 December 2018

Abstract

BACKGROUND CONTEXT: Posterolateral fusion (PLF) with autogenous iliac bone graft is one of the most common surgical procedures for lumbar spinal disease. However, its limited success demands new biologically competent graft enhancers or substitutes. Although the use of direct current (DC) electrical stimulation has been shown to increase rate of successful spinal fusions, little is known about the effect of the type of current in DC stimulation.

PURPOSE: To evaluate the effects of various DC stimulators on the strength and success rate of posterolateral fusion facilitated by using a nitinol mesh container, in rats.

STUDY DESIGN: This was an experimental animal study.

METHODS: A conductive, tubular nitinol mesh container was used to carry small pieces of bone grafts. The nitinol mesh container received electrical stimulation via a lead that connected the container to different types of DC stimulators. Sixty male Sprague-Dawley rats were divided into three groups (N=20 in each): a control group that underwent PLF with a nitinol container filled with autograft, a constant DC group that received a nitinol container and constant DC (100 μA), and a pulsed DC group that received a nitinol container and pulsed DC (100 μA, 100 Hz, 200 μs). The rats underwent PLF between L4 and L5, and transverse processes were grafted with bilateral iliac grafts. A stimulator was implanted subcutaneously. The rats were sacrificed 8 weeks postsurgery, and lumbar spines were removed. Spinal fusion was evaluated by microcomputed tomography, manual testing, biomechanical testing, histologic examination, and molecular analysis.

RESULTS: All animals in the DC stimulation groups displayed solid fusion, whereas only 70% of control animals showed solid fusion. Radiographic images, biomechanical testing, histologic examination, and molecular analysis revealed improved fusion in the order control group<constant DC group<pulsed DC group. The volume of new bone mass was significantly higher in the pulsed DC group ($p<.05$). Fusion was more solid in the pulsed DC group than in control group ($p<.05$). The pulsed DC group displayed the lowest inflammatory responses.

CONCLUSIONS: Pulsed DC electrical stimulation is efficacious in improving both strength and fusion rate in a rat spinal fusion model. In addition, tubular nitinol mesh, made of conductive suture, appears useful for holding small pieces of bone grafts and maintaining a good environment for bone fusion.

CLINICAL RELEVANCE: Pulsed DC electrical stimulation may be potentially useful to increase the fusion rate after spinal fusion in humans. Future research is required to evaluate the safety and efficacy of tubular nitinol mesh and pulsed DC electrical stimulation in humans.

FDA device/drug status: Not applicable.

Author disclosures: ***PGC***: Nothing to disclose. ***GYJ***: Nothing to disclose. ***YH***: Nothing to disclose. ***HYL***: Nothing to disclose. ***DAS***: Nothing to disclose.

PGC and GYJ contributed equally to this article and should be considered co-first authors.

* Corresponding author. Department of Neurosurgery, Yonsei University College of Medicine, 134 Shinchon-dong, Seodaemun-gu, Seoul, Republic of Korea. Tel.: (82)-2-2228-2150; fax: (82)-2-393-9979.

E-mail address: cistern@yuhs.ac (D.A. Shin).

https://doi.org/10.1016/j.spinee.2018.12.011
1529-9430/

Keywords: Constant direct current stimulation; Electrical stimulation; Human mesenchymal stem cell-like cells; Nitinol mesh; Osteogenic differentiation; Posterolateral fusion; Pulsed direct current stimulation

Introduction

Posterolateral fusion (PLF) surgery is the most common procedure for treating various spinal diseases [1–4]. The aim of PLF is to eliminate pain arising from instability of a motion segment or to prevent progression of deformity in patients with spinal instability or deformity, or degenerative lumbar spine disease. Autogenous bone grafting has been considered the gold standard for this purpose because autogenous bone grafts have osteoinductive, osteoconductive, and osteogenic properties [5]. However, there are several procedure-related complications associated with autografting, such as donor site pain, infection, and hematoma [6]. In addition, autografting cannot be used in certain cases, such as in (elderly) patients with poor bone quality, osteoporosis, or malignancy, or in case of a previously extracted donor site [7]. Although the application of pedicle screw fixation has improved the fusion rates, pseudoarthrosis occurs in nearly 40% of cases and reportedly causes persistent or recurrent pain and disability [8–10]. Therefore, for several decades, researchers have explored ways to enhance the fusion environment by mechanical or biological means [11–15]. However, such methods come with additional risks, and they have not completely eliminated pseudoarthrosis [16].

An alternative method to enhance the fusion environment is to apply direct current (DC) electrical stimulation. Electrical stimulation, which has been widely studied for its effect on bone healing, has an established role in the treatment of long-bone nonunions [17]. The clinical efficacy of electrical stimulation for spinal fusion was first reported by Dwyer et al. [18] in 1974. Several clinical studies showed that DC electrical stimulation enhances fusion success rates, particularly in "difficult to fuse" populations [19,20]. Meril reported the use of adjunctive DC stimulation of allograft bone in lumbar interbody fusions [21]. The DC-stimulated group had an overall success rate of 93%, compared with 75% in the nonstimulated group. Although DC electrical stimulation of spinal fusion has proven to be effective for increasing the fusion rates in "high-risk" patients, little information is available on the effect of the type of current used. The maintenance of a good healing environment for the maturation of bone fusion is important to increase the rate of spinal fusion. Prevention of soft-tissue interposition, easy migration of osteogenic cells, vascularization to the fusion mass core, and mechanical stress are important physiological factors that facilitate bone fusion [22]. The use of a protective graft container made of polylactide sheath has been demonstrated to enhance the fusion mass volume in a rabbit spinal fusion model [23]. Because of the undulating space between transverse processes, a flexible container that can be fixed closely to the transverse processes in PLF is preferred [24–26]. With the aim to enhance bone fusion, we used a flexible bone container made of a conductive tubular nitinol mesh that met the above-mentioned physiological requirements and we applied DC electrical stimulation in a rat PLF model. To assess the effect of the type of stimulation, we assembled two different types of DC stimulators. In addition, we investigated the biocompatibility of nitinol mesh container and varied DC stimulation during osteogenesis.

Materials and methods

Fabrication of nitinol mesh and electrical stimulators

Nitinol mesh (S&G Biotech, Seoul, Korea) (Fig. 1A), a flexible nickel-titanium alloy stent that is typically used in heart surgery, was used to transmit electrical stimulation and to collect bone chips. Regular quadrilaterals of 15 mm^2 were used in vitro, whereas cylindrical tubes of 15 mm in length and 6 mm in diameter and with a mesh size of 2 mm were used in vivo. The mesh size of the nitinol container was sufficiently large to allow cells to pass freely and thus allow good blood vessel growth, while preventing the interposition of soft tissue between bone grafts. Sources of electric current were LM334 (Texas Instruments, Dallas, TX, USA) and a lithium battery (CR2032 and CR2430; Energizer, St. Louis, MO, USA), which were used as power supplies (Fig. 1A). Two types of stimulators using DC electronic circuits provided a constant (100 μA) or pulsed (100 μA, 100 Hz, 200 μs) DC to the nitinol mesh (Fig. 1B). Brighton et al. [27] observed the highest fusion rate at a current of 100 μA in rats. In our preliminary study, 100 μA and 100 Hz showed the best results in vitro, and therefore, we used this current in this study. The stimulators were designed by Cybermedic (Iksan, Korea). Both the constant and the pulsed DC stimulator generated a mean voltage of 3V. The stimulators were coated with medical-grade silicone (NuSil, Carpinteria, CA, USA) to prevent the internal environment in vivo from getting exposed to electrical output and chemical byproducts created by the stimulator (Table 1).

Culture of human mesenchymal stem cell-like cells on nitinol mesh

To confirm the osteogenic effect of varied DC stimulation, and in vitro experiment was designed. Human mesenchymal stem cell-like cells (hMSC-LCs) were obtained from adipose tissue. hMSC-LCs were cultured in a 75 cm^2 flask containing MesenPro-RSTM basal medium (Thermo Fisher Scientific, Waltham, MA, USA), 2% growth supplement, and 2 mM L-glutamine (Thermo Fisher Scientific) at 37°C in a humid atmosphere with 5% CO_2. The medium was changed every 3 days, and subcultures were typically performed every 14 days. A Nitinol mesh was fixed to a Gosselin Petri dish (Gosselin, Corning, NY, USA) with four open compartments, which enables electron flow, and was then connected to the cathode and anode of either one of the DC stimulators (Fig. 2). The electrical stimulator delivered either constant

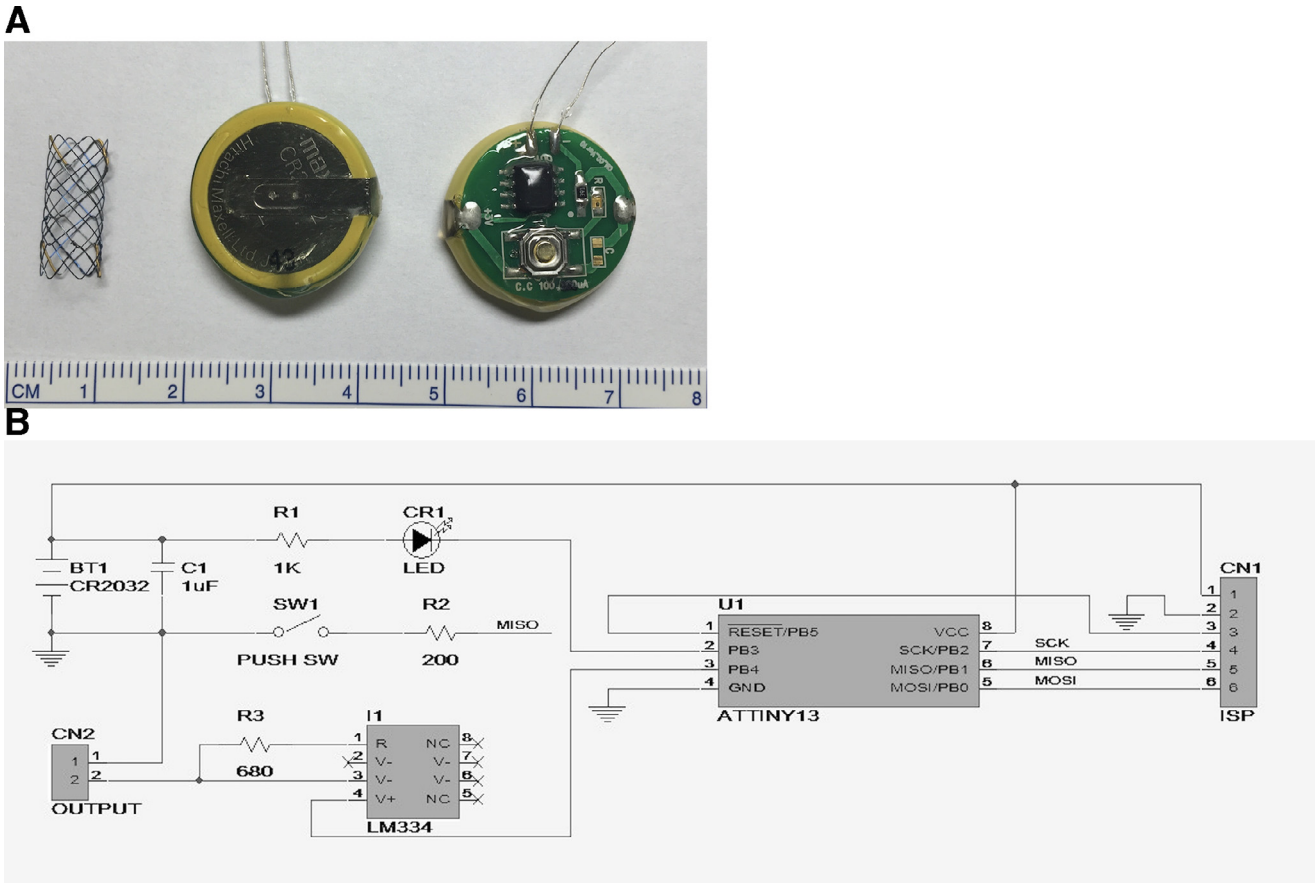

Fig. 1. A. Nitinol mesh and two electrical stimulators (left: bottom, right: top). B. Circuit diagram of electrical stimulator. Power button exists and status can be checked by LED lamp. C (capacitor) R (resister), V (voltage), SW (switch), PB (push button), GND (ground), VCC (supply voltage), SCK (serial clock), CR2032 (lithium battery), CR1 (LED lamp), LM334 (terminal adjustable current sources), ATTINY13 (AVR microcontroller), SCK (serial clock), MISO (master input, slave output), MOSI (master output, slave input).

(100 μA) or pulsed (100 μA, 100 Hz, 200 μs) DC to nitinol mesh for 4 weeks. Both the constant and the pulsed DC stimulator produced a mean voltage of 3 V through the nitinol mesh. hMSC-LCs were seeded on the nitinol mesh at a density of 5×10^4 cells. One day after cell seeding, the medium was changed to StemPro osteocyte differentiation basal medium (Invitrogen, Waltham, MA, USA) containing 5 μg/ml gentamicin to induce osteogenic differentiation. The medium was changed two times per week.

Characterization of human mesenchymal stem cell-like cells

Immunocytochemistry

hMSC-LCs were washed three times with Dulbecco's phosphate-buffered saline (DPBS; Gibco, Grand Island, NY, USA) for 5 minutes and were fixed with 4% paraformaldehyde for 30 minutes. After fixation, the cells were washed three times with phosphate-buffered saline, and incubated with DPBS containing 0.3% Triton X-100 (Sigma-Aldrich, St. Louis, MO, USA) for 10 minutes. The permeabilized cells were washed three times with DPBS for 5 minutes, incubated in DPBS containing 10% normal donkey serum (Jackson Laboratory, Barbor, ME, USA) for 1 hour, and incubated overnight with anti-CD90 (1:250, Abcam, London, UK), anti-CD44 (1:100, Abcam), anti-RUNX2 (10 μg/ml, Abcam), anti-osteocalcin (1:80, Abcam), anti-fibromodulin (5 μg/ml, Abcam), and antisclerostin (5 μg/ml, Abcam) at 4°C. After washing, the cells were incubated with secondary antibody conjugated with FITC or Cy3 for 1 hour. 4′,6-Diamidino-2-phenylindole-conjugated mounting medium (Vector Laboratories, Burlingame, CA, USA) was used to stain nuclei.

Alkaline phosphate staining

hMSC-LCs were washed with DPBS for 5 minutes and were fixed with fixative solution (2% citrate:acetone=2:3) for 30 seconds. After fixation, the cells were washed with distilled water for 1 minute. Then, the cells were stained with alkaline-dye mixture (fast blue RR salt, naphthol AS-Mx phosphate alkaline solution; Sigma-Aldrich) for 1 hour and washed three times with distilled water for 2 minutes. After washing, the cells were stained with Mayer's hematoxylin (Sigma-Aldrich) solution for 10 minutes and washed with distilled water for 3 minutes. The cells were dried for 2 days after removing moisture.

Table 1
Features of electrical stimulators

Item	Constant DC	Pulsed DC
Output current	100 μA	100 μA
Output waveform	Constant DC	Pulsed DC (100 Hz, 200 μs)
		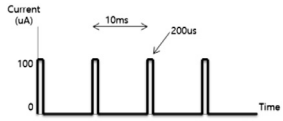
Load resistance (constant current)	0–20 kΩ	0–20 kΩ
Input voltage	Lithium battery 3 V (CR2032)	Lithium battery 3 V (CR2430)
Power consumption	0.36 mW (Output)	0.54 mW (Output), 0.45 mW (Sleep)
Effective time	10 wk	10 wk
Size	20×20×6 mm	25×25×6 mm
Molding	MED-6640 (NuSil, Carpinteria, CA, USA)	
Working condition	Works at 48 h after switch went on	

DC, direct current.

Alizarin red staining

hMSC-LCs were washed with DPBS for 5 minutes and were fixed with 10% formalin for 20 minutes. The cells were then washed three times with DPBS for 3 minutes. After washing, the cells were stained with 2% alizarin red solution (Sigma-Aldrich) for 5–30 minutes and washed three times with distilled water for 3 minutes. The cells were dried for 2 days after removing moisture.

Animal model and surgical procedure

This study was approved by the Institutional Review Board. We used 60 adult male Sprague Dawley rats (300± 15 g, mean±standard deviation; OrientBio, Gyeonggi-do, Korea), housed in an animal facility permitted by the Association for Assessment and Accreditation of Laboratory Animal Care. The rats were divided into three treatment groups: (1) fusion with nitinol container only as the control group; (2) fusion with nitinol container and application of constant DC (100 μA) as the constant DC group; and (3) fusion with nitinol container and application of pulsed DC (100 μA, 100 Hz, 200 μs) as the pulsed DC group (Table 2). The study was carried out by two neurosurgeons and one neuroscience postdoctoral researcher. Rats were anesthetized with intraperitoneal ketamine (100 mg/kg; Yuhan, Seoul, Korea) and xylazine (10 mg/kg; Rompun; Bayer, Leverkusen, Germany). Then, the animals were exposed to Isotroy 100 (Troikaa Pharmaceuticals Limited, Gujarat, India) and shaved, and the operation side was sterilized with 10% povidone-iodine solution. A dorsal midline incision was made, followed by two paramedian fascial incisions. An intermuscular plane between the multifidus and longissimus muscles was developed to expose the transverse processes of L4 and L5, as well as the intertransverse membrane. A low-speed drill was used to decorticate the transverse processes and expose cancellous bone. To harvest graft bones, a lateral oblique

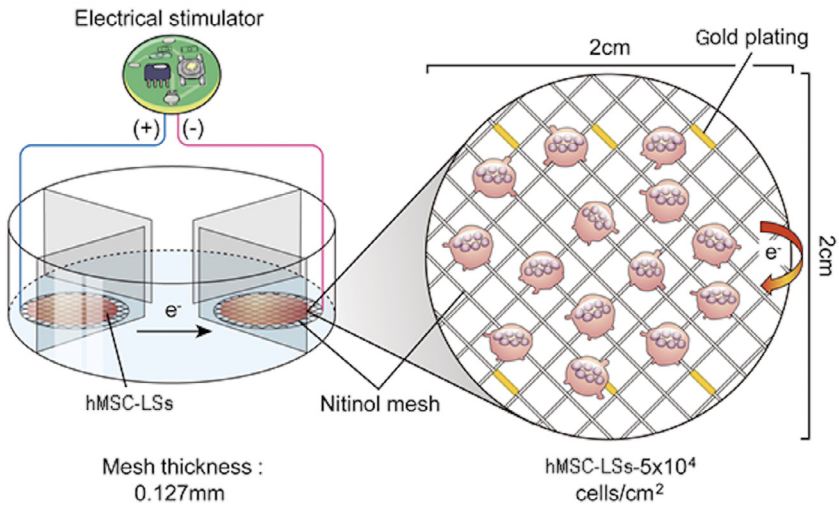

Fig. 2. Design of the chamber, nitinol mesh, and DC stimulation set-up. Illustration of osteogenic differentiation by DC stimulation in vitro using hMSC-LCs.

Table 2
Group description

Group	Graft materials	Number of rats
Control	Autologous bone+nitinol mesh	20
Constant DC	Autologous bone+nitinol mesh+ constant DC stimulator	20
Pulsed DC	Autologous bone+nitinol mesh+ pulsed DC stimulator	20

DC, direct current.

incision was made along the iliac crest on both sides. Then, all available corticocancellous bones were morselized with a rongeur and weighed to create a homogenous distribution of grafts between groups. The approximate weight of autologous iliac bone used in the control group was 300 mg. Autogenous bone graft was placed within a nitinol mesh (Fig. 3A). The nitinol mesh container was placed between decorticated transverse processes in the paraspinal bed (Fig. 3B). In the electrically stimulated groups of animals, a stimulator was placed subcutaneously. The wounds were closed with 3-0 nylon sutures. Rats recovered from anesthesia in warm basket for 15 minutes and were then returned to home cages. The nitinol mesh received electrical stimulation by means of a lead connecting the nitinol container to the DC generator. Two types of current density, constant (100 μA) and pulsed (100 μA, 100 Hz, 200 μs), were evaluated. DC current was applied to the nitinol container for 8 weeks. The animals were observed twice daily throughout the postsurgical study period for general attitude, appetite, appearance of the surgical site, neurological signs, and respiratory stress. Eight weeks after surgery, the rats were euthanized by ketamine overdose [28]. The lumbar spines from first lumbar vertebrae to sacral vertebrae, with surrounding musculatures intact, were explanted (Fig. 3C). The experimental design is outlined in Fig. 4. Spinal fusion was assessed by microcomputed tomographic (micro-CT) scan evaluation, manual testing, biomechanical testing, histologic examination, and molecular analyses. The two neurosurgeons who evaluated fusion were blinded to the treatments.

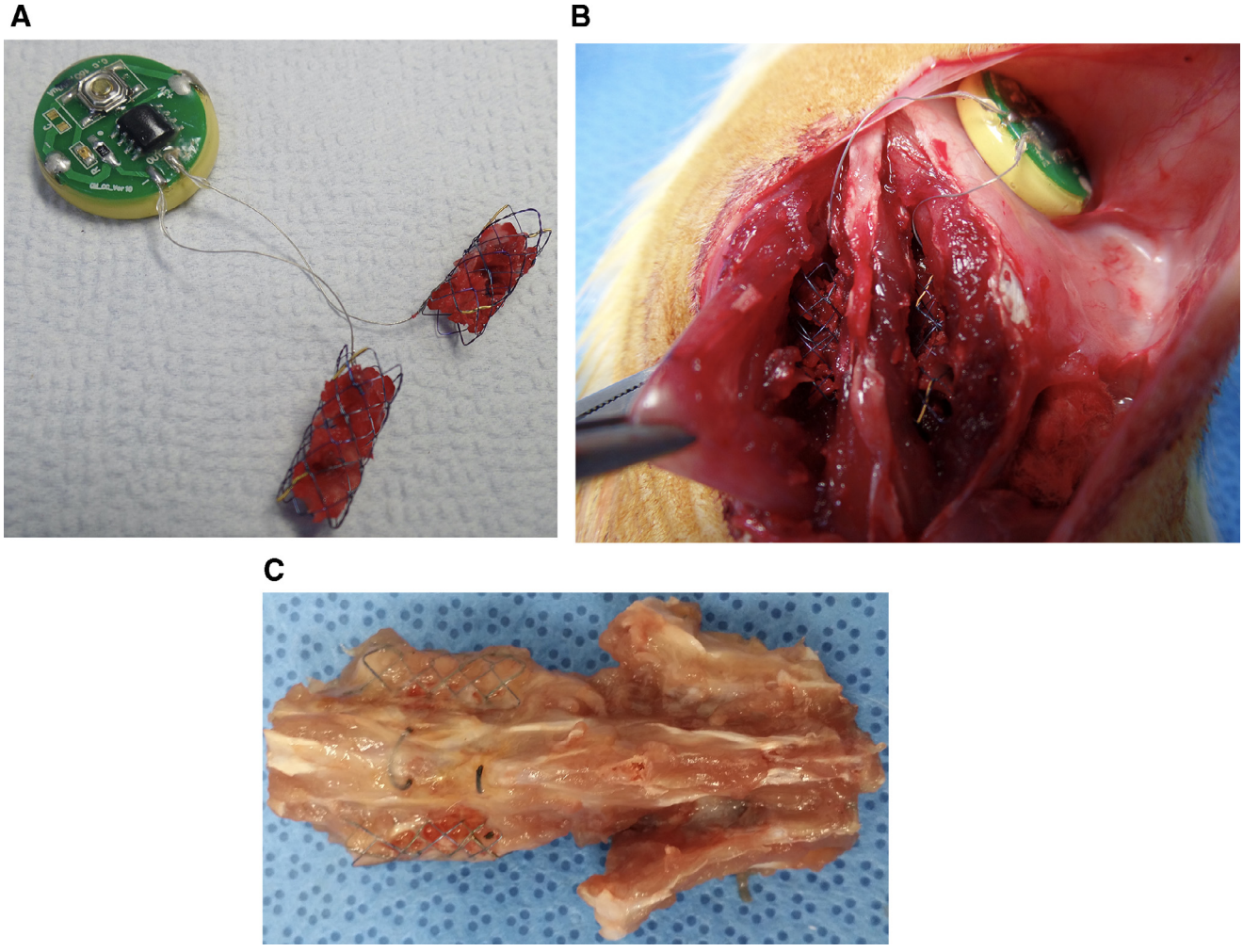

Fig. 3. A. A morselized iliac bone graft was placed inside a nitinol mesh, which was connected to an electrical stimulator. B. Two nitinol containers were implanted on posterior decorticated transverse process surfaces on both sides using one type of DC stimulator. C. Lumbar spine was extracted 8 weeks after surgery for fusion assessment.

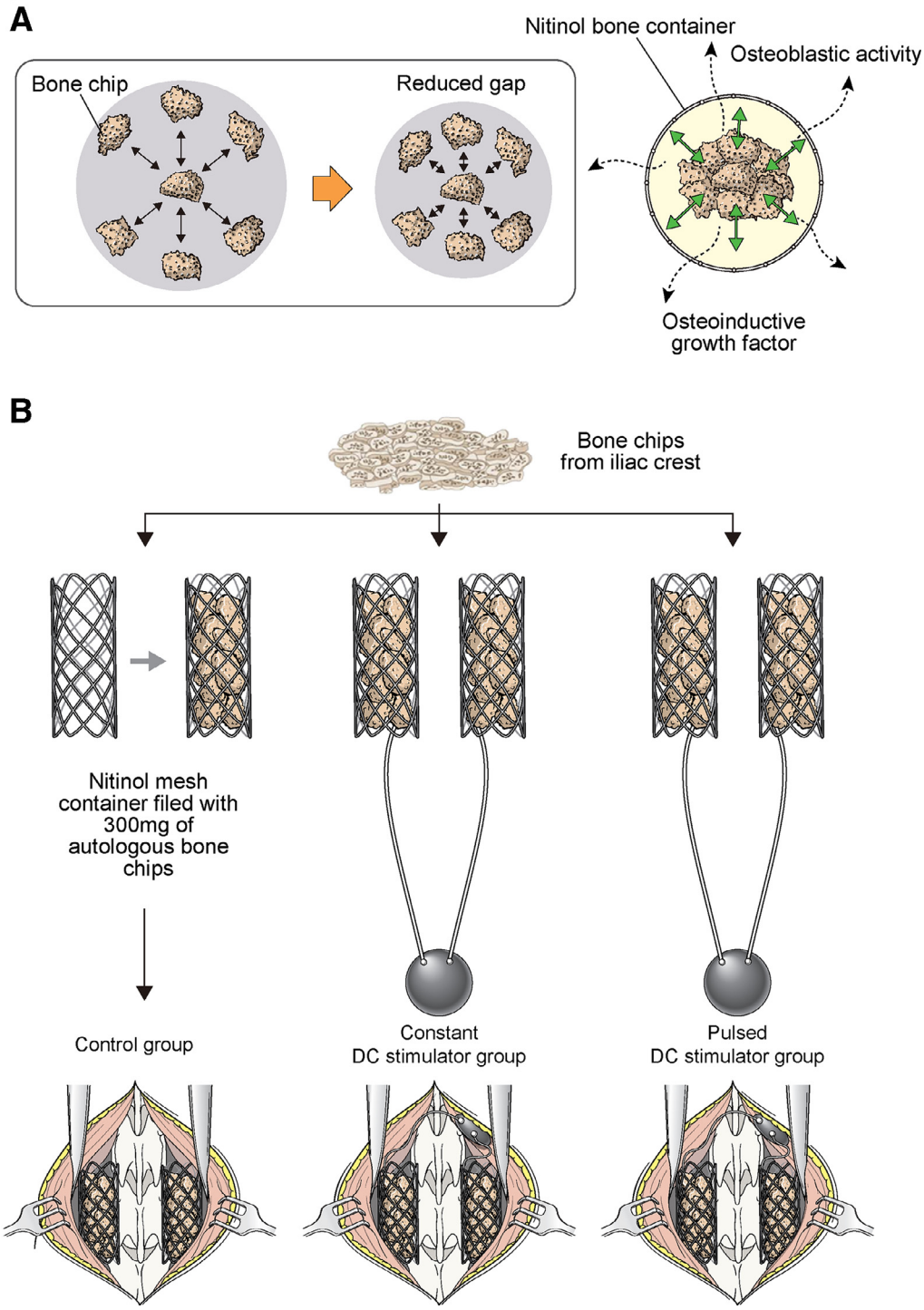

Fig. 4. Schematic illustration of rat posterolateral fusion. A. Nitinol mesh reduced gaps between bone chips and prevented soft-tissue interposition. B. Morselized corticocancellous bones were implanted in the space between L4 and L5 transverse processes using a nitinol mesh container with or without varied DC stimulator.

Microcomputerized tomography

The explanted spines were scanned by high-resolution micro-CT (NFR-Polaris-G90; NanoFocusRay, Jeonju, Korea) to measure calcified fusion mass at the region of PLF. Micro-CT scan was performed along the long axis of the spine, with an energy of 65 kVp, current of 115 μA, and exposure time of 34 ms to produce a resolution with a voxel size of 27.70 mm^3. Images were reconstructed using Feldkamp's cone-beam reconstruction algorithm [29]. The reconstructed image was 1024×1024 pixels, and 512 slices were acquired. Final data were converted to the Digital

Imaging and Communication in Medicine format. To investigate the integrity of the bone union, we examined scout, sagittal, and cross-sectional views by using Digital Imaging and Communication in Medicine viewer. We created three-dimensional image reconstructions to measure the total volume of fusion mass in both sides for each specimen, using commercial software (Xelis; INFINITT Healthcare, Seoul, Korea).

Gross palpation and manual testing

Lumbar spines were removed from the rats en bloc (Fig. 3C). Each fused motion segment was immediately palpated for continuity of the fusion mass between transverse processes. Two observers examined each manually segmented motion by flexion and extension at the fusion level and compared the motions to those of adjacent segments in the vertebral column. To prevent any mechanical damage to the fusion mass, the test was conducted carefully. Spines with no intersegmental motion were considered "solid," whereas spines with any motion detected on either side were defined as "not solid."

Biomechanical testing

The harvested specimens were evaluated in a three-point bending test using a TO-101 Universal Testing Machine (TESTONE, Seoul, Korea). Both ends of the vertebral body were placed with their dorsal sides down on two fulcra. The upper anvil (10.0 mm diameter) was placed in a position such that a load was applied on the ventral surface of the intervertebral disc perpendicular to the longitudinal spine. Three-point bending tests were performed at 40.0 mm intersupport distance and 50 mm/min crosshead speed until the upper anvil advanced to 10 mm (Fig. 5). The ultimate failure force was recorded as peak load to failure, and stiffness was calculated based on the slope of the linear portion of the force-displacement curve.

Histologic examination

Sample preparation

Explants were fixed in 10% neutral buffered formalin for 7 days. After washing, the samples were decalcified in EDTA at room temperature for 14 days. Decalcified specimens were used for histologic examination. The specimens were fixed in 10% neutral buffered formalin. After fixation, the specimens were dehydrated in graded ethyl alcohol solutions from 70% to 100%. Then, the specimens were then embedded in paraffin, and 4 μm thick sections were stained with hematoxylin and eosin (H&E) and Goldner's trichrome stains. The samples were immersed in a mixture of absolute ethanol and white resin (1:1, v/v), and then left on a rotor at room temperature for 1 hour. The ethanol/resin mixture was changed three times every hour. The samples were embedded in flat embedding molds made of polytetrafluoroethylene and cut on standard microtome using a motorized ultramicrotome and glass knife (5 mm).

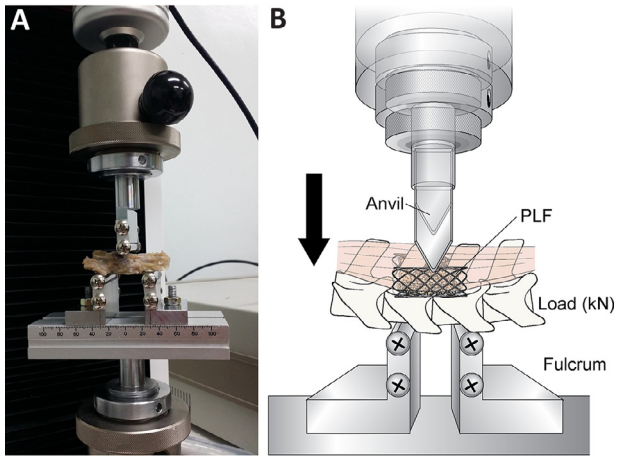

Fig. 5. Biomechanical assessment of fusion mass at 8 weeks after PLF by a three-point bending test. A. Experimental setup of the three-point bending test. B. The arrow indicates the direction of force exerted on the fusion mass.

Hematoxylin and eosin staining

Explants were sectioned at 20 μm thickness and the sections were stained with H&E. First, frozen section compounds (Leica, Wetzlar, Germany) were removed from each specimen. Nuclei were stained with hematoxylin at 37°C for 15 minutes and the sections were washed. Then, the tissues were differentiated in 0.35% acid alcohol solution, exposed to 1% lithium carbonate, and washed again. Next, the cytosol was stained with eosin for 5 minutes, followed by washing. Finally, the sections were dehydrated in graded ethanol (70%–100%), and cleared with xylene. The samples were mounted and observed under a light microscope (IX71; Olympus, Tokyo, Japan).

Goldner's trichrome staining

The sample was rinsed in xylene, 100% ethanol, 95% ethanol, and distilled water two times for 2 minutes. Then, the sample was placed in Bouin's fluid solution at 56°C for 1 hour. After rinsing with distilled water, the sample was placed in Weigert's hematoxylin for 10 minutes. The sample was then washed with tap water and stained with Ponceau Acid Fuchsin for 5 minutes. The sample was washed in 1% acetic acid and placed in Phosphomolybdic Acid Orange G solution (Sigma) until the collagen was decolorized. The sample was rinsed with 1% acetic acid, stained in light green stock solution for 5 minutes, and rinsed with 1% acetic acid. The samples were mounted and observed under a light microscope (IX71; Olympus, Tokyo, Japan).

Immunohistochemistry

Sections were incubated with primary antibody in incubation buffer (1% bovine serum albumin, 1% normal donkey serum, 0.3% Trion X-100, and 0.01% sodium azide in

PBS) at 4°C overnight, and then with secondary species-specific fluorescently labeled antibodies at room temperature for 1 hour. Then, the sections were mounted with mounting solution (UltraCruz Mounting Medium, Santa Cruz Biotechnology, Dallas, TX, USA) and observed under a laser confocal microscope (LSM 510; Zeiss, Gottingen, Germany) and a Leica microscope (DM 2500; Leica, Wetzlar, Germany).

Molecular analysis

The L4 and L5 segments, which had been fused with the nitinol mesh and varied DC stimulator, were collected and stored at −80°C until analysis. The surrounding soft tissue was removed and the bone was placed on a dry ice block. The bone was pulverized in liquid nitrogen to near-powder state using a mortar and pestle. The powder was transferred to an Eppendorf tube, RIPA lysis buffer (Thermo, Waltham, MA, USA) supplemented with protease/phosphatase inhibitors (Thermo) was added, and the sample was left on ice for 15 minutes. Then, the sample was centrifuged at 13,000×*g* for 15 minutes.

The differentiation of hMSC-LCs by electrical stimulation was analyzed by western blotting. Detached cells were lysed and the proteins in the lysates were resolved by 10%−12% SDS-PAGE (Bio-Rad, Richmond, CA, USA) and electroblotted onto PVDF membranes. After blocking, the membranes were incubated with primary antibodies targeting Bcl-2-associated X (Bax; dilutions of 1:1,000; Millipore Corp., Milford, MA, USA) and β-actin (1:10,000; Abcam, Cambridge, UK). After conjugation of secondary antibodies, protein signals were detected using an automatic radiograph film processor (TM-300E; TAEAHN Inc., Incheon, Korea) and quantified using ImageJ (NIH, Bethesda, MD, USA). We used antiosteocalcin, anticollagen type1, anti-CD90, and anti-CD44.

Statistical analysis

All quantitative data are presented as the mean±standard deviation. Group means were compared by one-way ANOVA. A p value of less than .05 was considered statistically significant. All statistical analyses were performed using SPSS Statistics software, Version 21.0 (IBM, Somers, NY, USA).

Results

Pulsed DC stimulation improves bone formation in vitro

To evaluate the effect of constant or pulsed electrical stimulation on osteogenic differentiation, hMSC-LCs positive for both CD44 and CD90 were cultured in a specifically designed compartmentalized dish and were observed for 4 weeks. Three-dimensional cell masses grew over a week, with particularly significant growth in the pulsed DC group (Fig. 6A). The differentiation of hMSC-LCs was also compared by means of immunostaining. When hMSC-LCs originally positive (green color) for CD90 began to differentiate at 1 week, they were no longer CD90 positive, but expressed RUNX2 (red color), a preosteoblast marker (Fig. 6B). After 4 weeks, the cells stained positive for osteocalcin, a marker of mature osteoblasts (Fig. 6B). Alkaline phosphate staining did not produce signal in the first week, but after 4 weeks, violet-stained osteoblasts were clearly observed (Fig. 6C). Especially cells near the nitinol mesh were observed to be stained, in both constant and pulsed DC groups (Fig. 6C). Furthermore, the remarkable formation of bone mass adjacent to the negative terminal indicated a strong correlation between bone formation and electrical stimulation. After 4 weeks, significantly more osteocytes were observed in the pulsed DC group than in the other groups in an alizarin red staining test. (Fig. 6D).

Microcomputerized tomography

In the in-vivo experiment, micro-CT images revealed that the pulsed DC group showed more extensive new bone formation in the fusion mass at 8 weeks after PLF ($p<.05$). Fusion masses in both the DC groups were fused firmly with adjacent transverse processes, and no cracks were observed inside the fusion masses (Fig. 7A). On the other hand, although the control group also showed new bone formation, clefts were observed between the L4 and L5 transverse processes. Unremodeled bone chips were also noted in both DC groups; however, cortical rims were better defined than those in the control group. The volume of new bone mass varied significantly between the groups, and was 277.6±8.5 mL, 263.5±11.8 mL, and 225.4±20.1 mL in the pulsed DC, constant DC, and control group, respectively ($p<.05$, Fig. 7B). In addition, the sizes of fusion masses at the right side of the transverse process, near the negative terminal, were statistically significantly different between the groups (138.4±6.7 mL, 134.6±7.5 mL, and 101.7±14.8 mL in pulsed DC, constant DC, and control group, respectively; $p<.05$, Fig. 7B).

Manual assessment of fusion

Manual palpation at 8 weeks after PLF revealed that 90% (54/60) of the explanted spines displayed solid fusion. Six rats with “not-solid” fusion, all of which belonged to the control group, showed less bony mass on gross inspection and intersegmental motion on manual palpation. In all rats with solid fusion, continuous bony mass was observed by palpation and no intersegmental motion was noted between intertransverse processes. The control group had a solid fusion rate of only 70% (14/20), whereas both DC groups showed complete fusion in all cases (100%, 40/40; $p<.01$). Extended bony growth invading paravertebral muscle dorsally and psoas muscle ventrally was not observed.

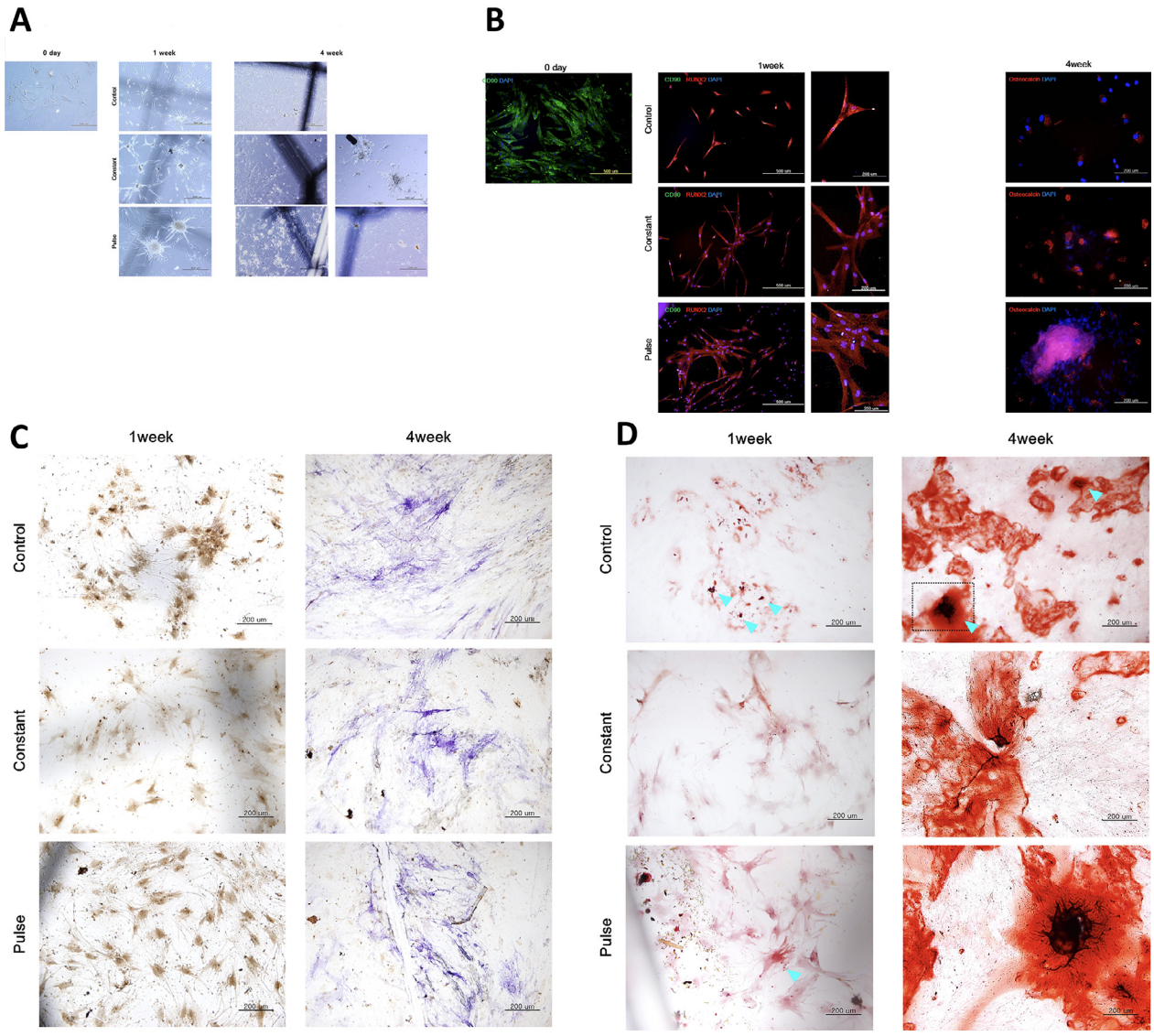

Fig. 6. Pulsed DC stimulation improves bone formation in vitro. A. Microscopic images of hMSC-LCs cultured on nitinol mesh. The pulsed DC stimulator group showed significant growth of cell mass, especially near the negative electrode. B. Immunostaining of cultured cells of the various treatment groups. C. Alkaline phosphate staining. Osteoblasts are stained violet. Staining was not detected in 1 week. After 4 weeks, prominent staining was observed. Cells near the nitinol container were stained in both the constant and the pulsed DC groups. D. Alizarin red staining. Osteocytes are stained red. The pulsed DC group showed the most extensive growth along the negative nitinol wire.

Biomechanical testing

Biomechanical testing was performed to evaluate peak force to failure and stiffness, as determined on the basis of the force-displacement slope. L4–L5 segments of all treatment groups were tested and analyzed individually. The ultimate force required to cause bone fracture was the greatest in the pulsed DC group, with 239.46±35.40 N ($p<.05$). The levels of force measured in the control group and constant DC group were 143.17±72.60 N and 180.68±36.22 N, respectively (Fig. 8A). In comparison to 16.1±10.6 N/mm in the control group, bones in the constant DC group demonstrated greater stiffness of 23.8±4.4 N/mm, and those in the pulsed DC group showed even greater stiffness of 31.9± 6.2 N/mm, which was significantly different from that in the control group ($p<.05$; Fig. 8B). Stiffness showed a trend very similar to that of the ultimate force test results.

Histologic examination

Fusion masses were evaluated by immunohistochemistry, H&E staining, and Goldner's trichrome staining. Osteocalcin and sclerostin were visualized by immunohistochemistry. Osteocalcin is used as a preliminary biomarker of bone formation. Unexpectedly, osteocalcin was the most abundant in the control group. The pulsed DC group showed higher osteocalcin levels and lower inflammation than the constant DC group (Fig. 9A, C). Sclerostin, which is produced by osteocytes, has antianabolic effects on bone formation. Osteocytes are generally acknowledged to sense loading

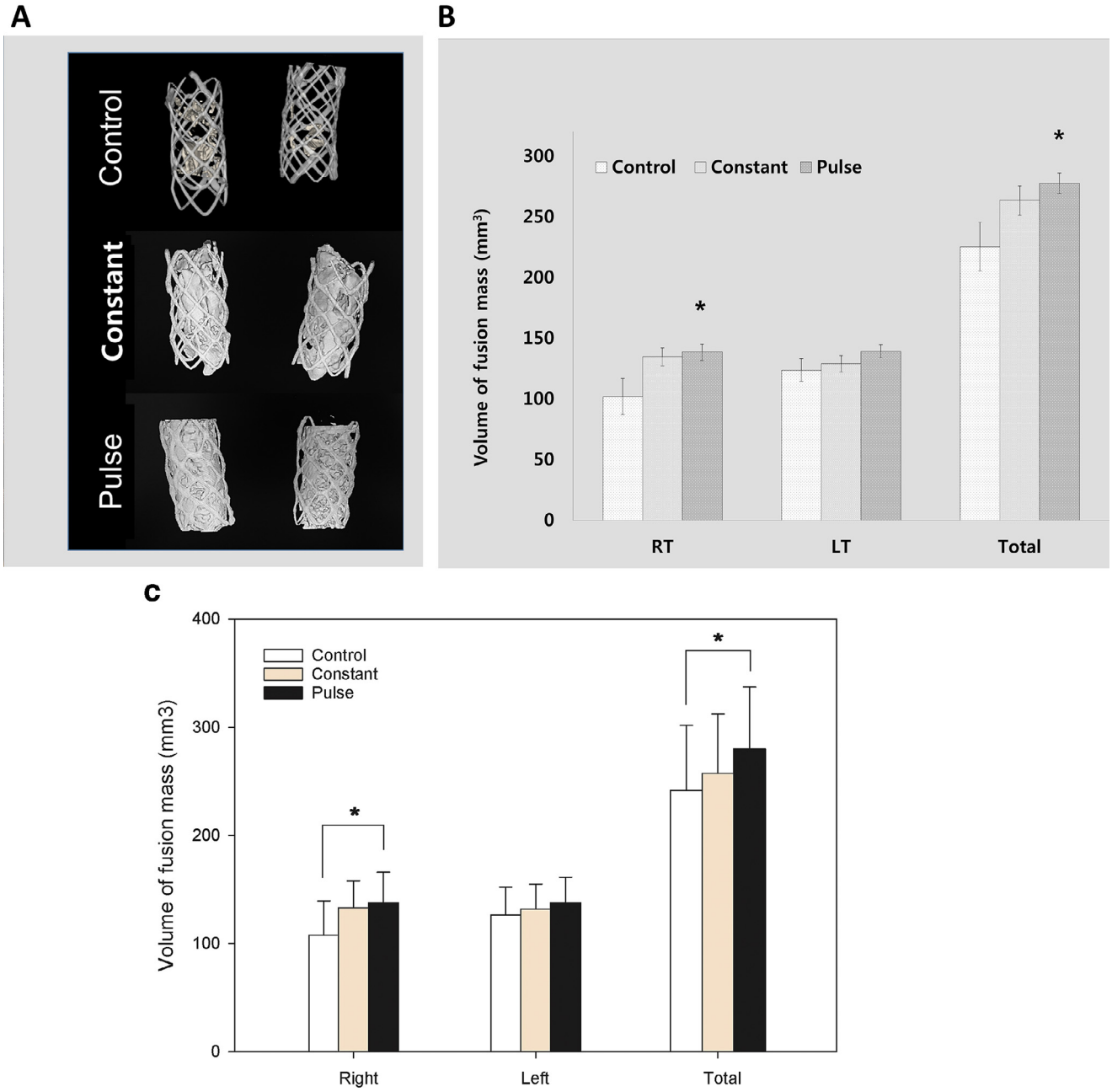

Fig. 7. Microcomputed tomography analysis of newly formed bone mass at 8 weeks after PLF. A. Three-dimensional microcomputed tomography images revealing the volume of new bone mass. B. Graph illustrating the volume of fusion mass. Rt is the (−) polar site and Lt is the (+) polar site. Data are the mean±SD. *p<.05 versus control.

stimuli and to regulate bone remodeling and turnover. Sclerostin was considerably observed in both the constant and the pulsed DC group (Fig. 9B). Spinal fusion was observed in all three groups by H&E staining. The pulsed DC group showed higher bone union with peripheral bone than other groups. Disintegration of paravertebral tissue was higher in the constant DC group than in the pulsed DC group. Such disintegration was supposed to have resulted from inflammation induced by constant DC stimulation (Fig. 9C). In the constant DC group, inflammation was observed in the bone mass and paravertebral tissue around the stent. In Goldner's trichrome staining, solid fusion was observed along the nitinol mesh and decorticated transverse processes in all three groups. Osteoid showed a trend very similar to that of H&E staining results; we observed newly formed, unmineralized "bone-like" dense collagen fibers (osteoid), which would eventually mature and mineralize to form bones (Fig. 9D).

Molecular analysis

Osteocalcin and sclerostin protein levels in bone tissues were analyzed at 8 weeks after PLF by western blotting

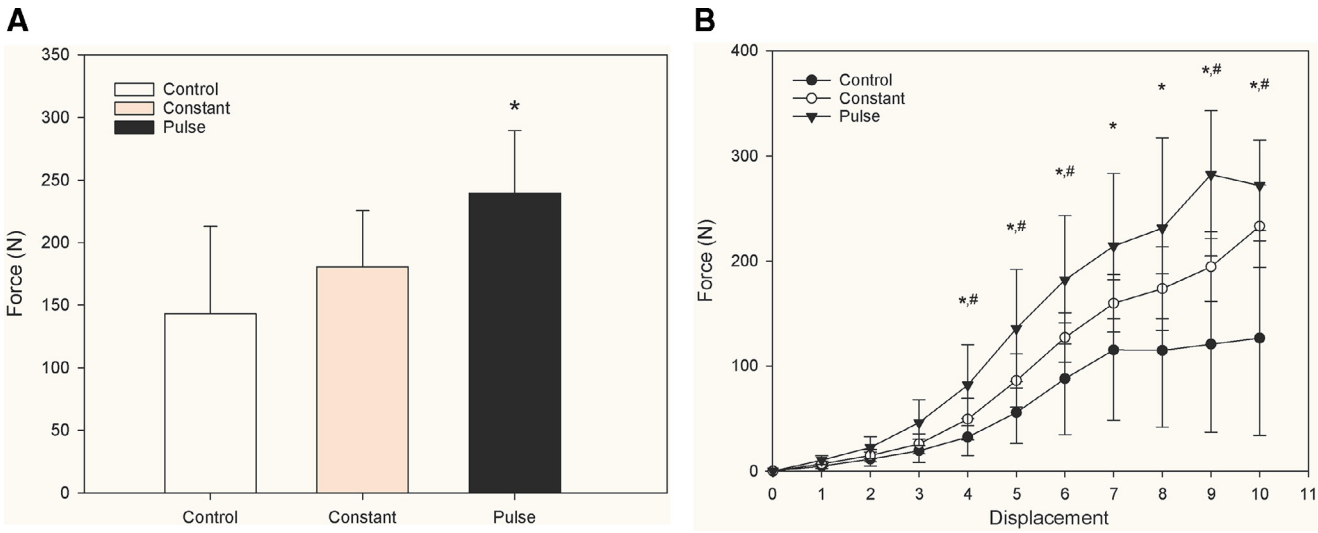

Fig. 8. Biomechanical assessment of fusion mass at 8 weeks after PLF by three-point bending test. A. Average ultimate force to failure of fusion mass for each treatment group. The amount of force required to cause fracture was greater in the pulsed DC group than in the control and constant DC groups. *p<.05 versus control. B. Force-displacement curves of fusion mass for each group. Pulsed DC group showed greater stiffness than both control and constant DC groups. Data are the mean ± SD. *p<.05 versus control. #p<.05 versus constant DC.

(Fig. 10A). Protein expression was normalized to the amount of β-actin, which was set as 1. The relative expression of osteocalcin was 0.83, 0.49, and 0.8 in the control, constant DC, and pulsed DC group, respectively, with no significant difference between the control and pulsed DC groups. The relative expression of sclerostin was 0.77, 0.85, and 0.9 in the control, constant DC, and pulse DC group, respectively (Fig. 10B). These results indicated that at 8 weeks after PLF, when pulsed electrical stimulation was applied, osteocytes were more prominently induced.

Discussion

Attainment of reliable fusion is the most important prognostic factor for clinical success in PLF surgery. In conventional spinal fusion surgeries, certain risk factors, such as old age, smoking, multiple-level fusion, and failed prior surgery, have been found to affect the fusion rate [30]. In particular, the elderly display less solid fusion despite the use of autograft, as this population has more diabetes, malnutrition, and poor bone quality due to osteoporosis [31]. Therefore, alternative methods, such as synthetic graft substitutes, tissue-engineered alternatives, tubular mesh containers, and electrical stimulation have been designed for use as adjuncts to spinal fusion surgery [26,32,33].

For more than 30 years, electrical stimulation has been used to enhance spinal fusion [20,32]. Since the earliest reported clinical use of electrical stimulation, both clinical and scientific studies on electrical stimulation have increased in numbers. In 1974, Dwyer et al. [18] published the usefulness of electrical stimulation in high-risk patients. Kane et al. [19] published a study on implantable electrical stimulation in 1988. Rogozinski et al. [20] showed that implantable electrical stimulation resulted in a high rate of fusion in high-risk patients (96 % vs. 85 %) in 1996. Kucharzyk et al. [34] carried out a controlled prospective outcome study of implantable electrical stimulation in high-risk instrumented spine fusion and reported a fusion rate of 95.6% compared with 85% in those not receiving electrical stimulation. Among the reported techniques, DC electrical stimulation is the most widely used [34–36].

This study aimed to investigate the effects of various DC stimulation on new bone formation, osteo-inductivity, and biologic response to PLF using a nitinol mesh container in a rat PLF model. Conventional PLF involves meticulous decortications of transverse processes as well as piece-by-piece placement of autografts in the intertransverse spaces; consequently, it does not guarantee close contact between transverse processes and graft pieces. To remedy this problem, we prepared a flexible container made of conductive tubular nitinol mesh that facilitated contact with irregular recipient bone surfaces and provided strong tensile strength. As a container that holds bone pieces together, the mesh served as a “fusion environment keeper.” Nitinol, which maintains a good healing environment for bone fusion, is currently the preferred option for clinical application that eliminates concerns of graft-induced complications. Therefore, tubular nitinol mesh may be a promising tool for promoting spinal fusion [26]. Radiographic images, biomechanical testing, as well as histologic and molecular analyses demonstrated an increase in the fusion rate when the pulsed DC stimulator was used in combination with nitinol container, compared with when only nitinol container with autograft was used. Although new bone formation was observed in all three treatment groups, new bone volume and strength increased in the order control group>constant DC group>-pulsed DC group. Furthermore, solid fusion was achieved in all cases of both DC group, whereas only 70% of cases in the

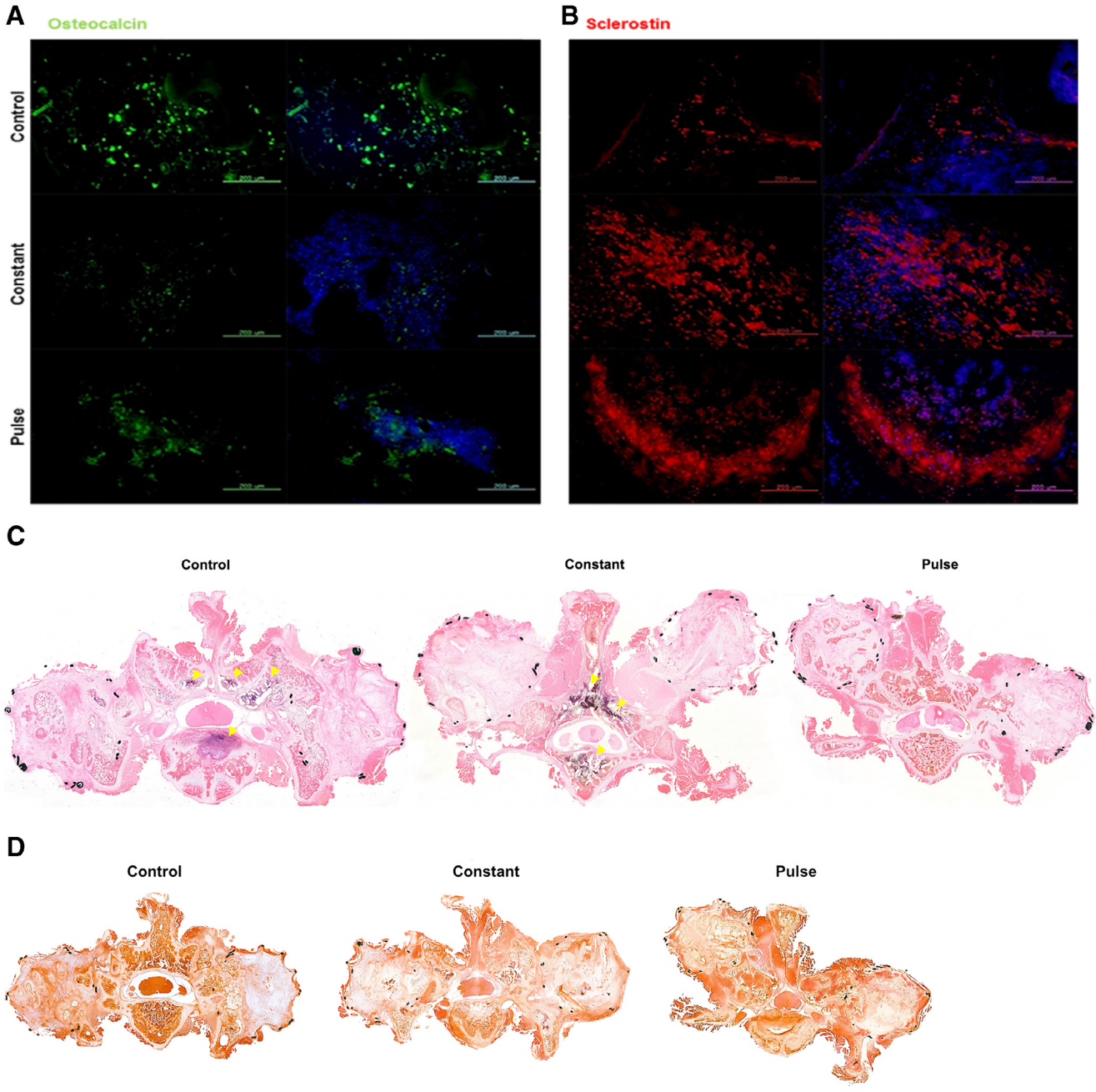

Fig. 9. Histologic staining of fusion mass at 8 weeks after PLF. Control, constant, and pulsed groups are shown from left to right. A. Mature osteoblasts stained by antiosteocalcin (green). B. Osteocytes stained by antsclerostin (red). C. Hematoxylin and eosin (H&E) staining shows inflammation in the center of spine in constant group (yellow arrow: inflammation region). D. Goldner's trichrome staining shows mature and circuitous osteoid structure (orange color: osteoid region).

control group displayed solid fusion. These figures imply that using DC stimulation further improves spinal fusion and the quality of osteogenesis achieved with a nitinol container. These results are encouraging because the use of DC stimulation with nitinol container might reduce the chance of pseudoarthrosis or nonunion, which is reported to occur in 5%–45% of conventional spinal fusion procedures [37,38]. The use of adjunctive electrical stimulation to enhance the healing of spinal fusion has been shown to be efficacious in both clinical and experimental settings [39].

The mechanism by which DC stimulation stimulates osteogenesis has been studied using several animal models. A previous study on dogs demonstrated statistically significantly higher fusion rates in DC stimulated specimens by 12 weeks [40]. In addition, DC stimulation reportedly enhances fusion success rates in a dose-dependent manner. In a rabbit model using DC in combination with coral-derived bone substitute as an alternative to autograft, Bozic et al. [41] showed that 100 μA stimulation combined with coral was superior to autograft. Kahanovitz et al. [42]

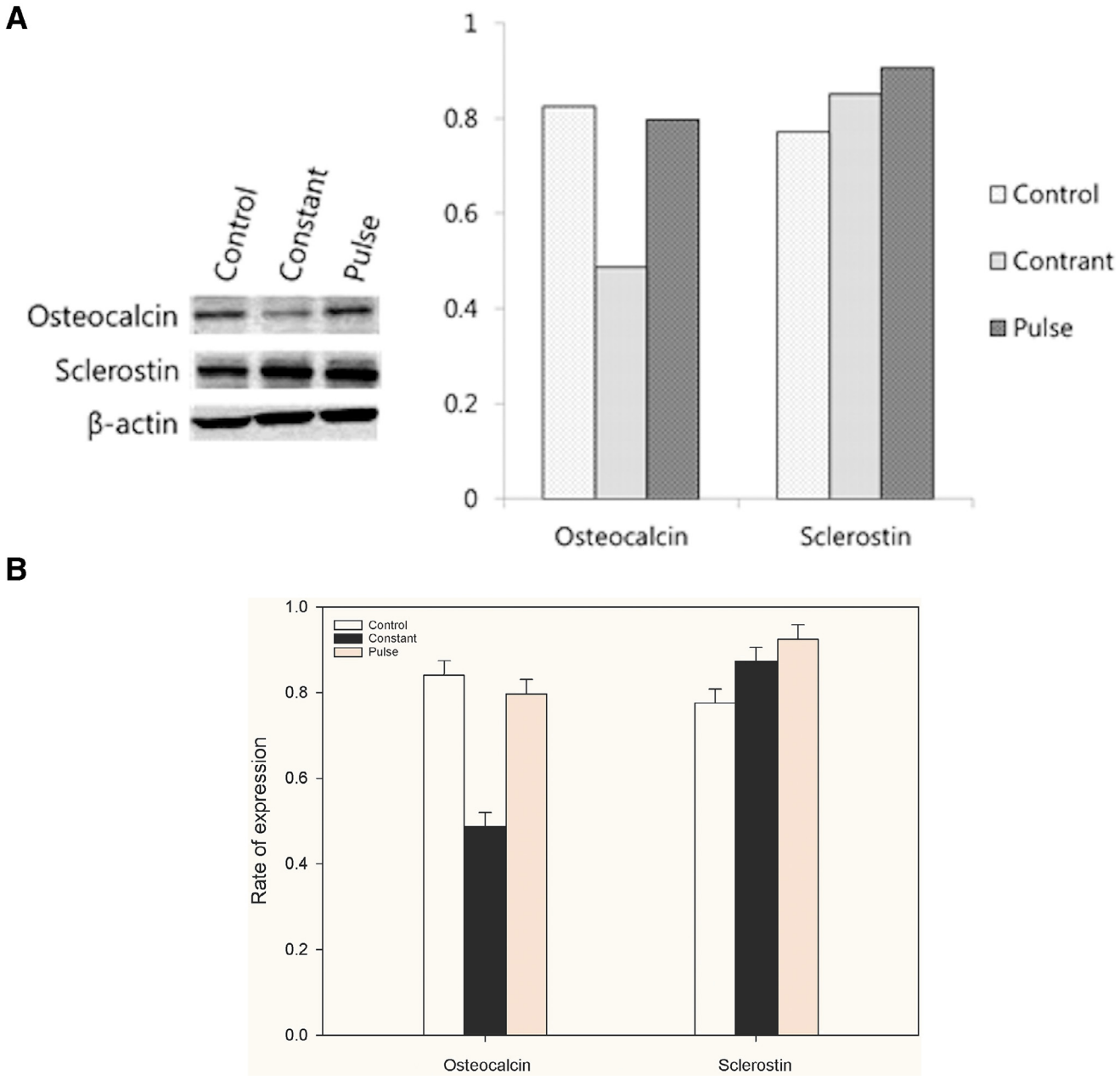

Fig. 10. Protein analysis of of fusion mass at 8 weeks after PLF. A. Western blot for osteocalcin and sclerostin. B. Expression of osteocalcin and sclerostin relative to that of β-actin. Osteoblasts were prominent in the control group. Electrical stimulation promoted osteocytes in the constant and pulsed DC groups compared with the control group, with pulsed DC having a stronger effect than constant DC.

developed a facet fusion canine model to show that DC stimulation increases the fusion success rate and shortens the time to fusion in a dose-dependent fashion. Similar results were obtained in a pig model [43]. However, an authentic electrical current stimulator that can provide optimal fusion outcome without tissue necrosis has yet to be determined. It has been hypothesized that pulsed stimulation, which resembles physiological signals in the human body such as human heartbeat and synaptic nerve stimuli, delivered to fusion site would result in solid fusion, while having less adverse effects on contiguous bony and soft tissues. This study is the first to provide evidence that pulsed DC stimulation can be used to enhance fusion success. Unlike constant DC stimulation, pulsed DC stimulation will not only facilitate effective fusion of damaged bone mass, but also minimize harmful factors that contribute to inflammatory reactions around the fusion mass, as supported by our high-resolution histologic examination findings. In the pulsed DC group, no evidence of inflammation and necrosis was found within the fused mass at the stent or near spinous processes. The histologic data, which revealed that the pulsed DC group showed increased bony ingrowth and resorption of the autograft in the nitinol container compared with the other groups, were consistent with biomechanical test results.

The fabrication of tubular nitinol container is very simple compared with that of other, similar containers, which usually cost more and require advanced technology. We used a conductive tubular nitinol mesh that is approved by the Korea Food and Drug Administration. Nitinol mesh has been used for repairing various types of organs, joints, and tissues, and triggers low immunological responses [44–47].

In the current study, the electrode was inserted into the subcutaneous space. Brighton et al. [27], in their study in 1989, confirmed that the weight per unit volume of osteoporotic vertebral bodies in castrated rats increased through transcutaneous electrical stimulation with a 100 mA current. However, it is difficult to accurately identify the effect of electrical stimulation to the bone due to electrical impedance of the skin and bone. Therefore, to avoid the impedance issue, we inserted the implant into the body to efficiently deliver the current to the bone. However, in humans, the electrode implant should be removed after fusion. In some previous human studies, the effect of transcutaneous electrical stimulation on spine fusion has been confirmed. Goodwin et al. [48], Mooney et al. [36], and Linovitz et al. [49] have shown that transcutaneous electrical stimulation after spine fusion increases the fusion rate. In humans, both implanted and transcutaneous electrodes are options. It is expected that transcutaneous electrodes would be more convenient; however, research on impedance, uniform current transmission, and wearing is needed.

Although this study provided novel information regarding the use of various types of DC stimulation with a nitinol container for PLF, it had several limitations. First, the spinal biomechanics in a tetrapod animal model differ significantly from those observed in humans. In future studies, a higher-order animal model should be used to assess the effect of these interventions on spinal fusion rates in primates. Second, the accuracy and extent of interobserver agreement for manual palpation testing and radiographic technique were not extensively evaluated in this preclinical model. Third, inconsistencies in the surgical methods might have led to fusion outcome bias. Fourth, we used a continuous and pulsed DC current of 100 mA based on previous studies. At this current, the pulsed mode induced better fusion and less inflammatory reaction and necrosis. However, other DC currents may induce other effects, and more research is needed.

Conclusions

Tubular nitinol mesh, made of conductive suture, appears useful for holding small pieces of bone grafts and maintaining an environment conducive to bone fusion. This study showed the benefits of using pulsed DC electrical stimulation in a rat spinal fusion model. Pulsed DC stimulation was superior to constant DC stimulation in terms of fusion rate, fusion strength, and suppression of inflammatory reactions. Future research is required to evaluate the safety and effectiveness of electrical stimulation in humans.

Acknowledgment

This work was supported by the National Research Foundation of Korea (NRF) grant funded 50 thousand dollars by the Korea government (MEST) (no. 2013027782).

References

[1] Boden SD. Overview of the biology of lumbar spine fusion and principles for selecting a bone graft substitute. Spine 2002;27(16 Suppl 1): S26–31.
[2] Gertzbein SD, Hollopeter M, Hall SD. Analysis of circumferential lumbar fusion outcome in the treatment of degenerative disc disease of the lumbar spine. J Spinal Disord 1998;11:472–8.
[3] Rompe JD, Eysel P, Hopf C. Clinical efficacy of pedicle instrumentation and posterolateral fusion in the symptomatic degenerative lumbar spine. Eur Spine J 1995;4:231–7.
[4] Herkowitz HN, Sidhu KS. Lumbar spine fusion in the treatment of degenerative conditions: current indications and recommendations. J Am Acad Orthop Surg 1995;3:123–35.
[5] Flouzat-Lachaniette CH, Ghazanfari A, Bouthors C, Poignard A, Hernigou P, Allain J. Bone union rate with recombinant human bone morphogenic protein-2 versus autologous iliac bone in PEEK cages for anterior lumbar interbody fusion. Int Orthop 2014;38:2001–7.
[6] Ito Z, Imagama S, Kanemura T, Hachiya T, Miura Y, Kamiya M. et al. Bone union rate with autologous iliac bone versus local bone graft in posterior lumbar interbody fusion (PLIF): a multicenter study. Eur Spine J 2013;22:1158–63.
[7] Emery SE, Hughes SS, Junglas WA, Herrington SJ, Pathria MN. The fate of anterior vertebral bone grafts in patients irradiated for neoplasm. Clin Orthop Relat Res 1994;27:207–12.
[8] Boden SD, Martin Jr. GJ, Morone M, Ugbo JL, Titus L, Hutton WC. The use of coralline hydroxyapatite with bone marrow, autogenous bone graft, or osteoinductive bone protein extract for posterolateral lumbar spine fusion. Spine 1999;24:320–7.
[9] Fu TS, Chen WJ, Chen LH, Lin SS, Liu SJ, Ueng SW. Enhancement of posterolateral lumbar spine fusion using low-dose rhBMP-2 and cultured marrow stromal cells. J Orthop Res 2009;27:380–4.
[10] Nakajima T, Iizuka H, Tsutsumi S, Kayakabe M, Takagishi K. Evaluation of posterolateral spinal fusion using mesenchymal stem cells: differences with or without osteogenic differentiation. Spine 2007;32: 2432–6.
[11] Taghavi CE, Lee KB, Keorochana G, Tzeng ST, Yoo JH, Wang JC. Bone morphogenetic protein-2 and bone marrow aspirate with allograft as alternatives to autograft in instrumented revision posterolateral lumbar spinal fusion: a minimum two-year follow-up study. Spine 2010;35:1144–50.
[12] Ajiboye RM, Hamamoto JT, Eckardt MA, Wang JC. Clinical and radiographic outcomes of concentrated bone marrow aspirate with allograft and demineralized bone matrix for posterolateral and interbody lumbar fusion in elderly patients. Eur Spine J 2015;24:2567–72.
[13] Virk S, Sandhu HS, Khan SN. Cost effectiveness analysis of graft options in spinal fusion surgery using a Markov model. J Spinal Disord Tech 2012;25:E204–10.
[14] Hoffmann MF, Jones CB, Sietsema DL. Adjuncts in posterior lumbar spine fusion: comparison of complications and efficacy. Arch Orthop Trauma Surg 2012;132:1105–10.
[15] Thalgott JS, Giuffre JM, Fritts K, Timlin M, Klezl Z. Instrumented posterolateral lumbar fusion using coralline hydroxyapatite with or without demineralized bone matrix, as an adjunct to autologous bone. Spine J 2001;1:131–7.
[16] Bernhardt M, Swartz DE, Clothiaux PL, Crowell RR, White 3rd AA. Posterolateral lumbar and lumbosacral fusion with and without pedicle screw internal fixation. Clin Orthop Relat Res 1992(284):109–15.

[17] Brighton CT, Black J, Friedenberg ZB, Esterhai JL, Day LJ, Connolly JF. A multicenter study of the treatment of non-union with constant direct current. J Bone Joint Surg Am Vol 1981;63:2–13.
[18] Dwyer AF, Wickham GG. Direct current stimulation in spinal fusion. Med J Aust 1974;1:73–5.
[19] Kane WJ. Direct current electrical bone growth stimulation for spinal fusion. Spine 1988;13:363–5.
[20] Rogozinski A, Rogozinski C. Efficacy of implanted bone growth stimulation in instrumented lumbosacral spinal fusion. Spine 1996; 21:2479–83.
[21] Meril AJ. Direct current stimulation of allograft in anterior and posterior lumbar interbody fusions. Spine 1994;19:2393–8.
[22] Boden SD. Biology of lumbar spine fusion and use of bone graft substitutes: present, future, and next generation. Tissue Eng 2000;6:383–99.
[23] Poynton AR, Zheng F, Tomin E, Lane JM, Cornwall GB. Resorbable posterolateral graft containment in a rabbit spinal fusion model. J Neurosurg 2002;97(4 Suppl):460–3.
[24] Abduljabbar FH, Makhdom AM, Rajeh M, Tales AR, Mathew J, Ouellet J, et al. Factors associated with clinical outcomes after lumbar interbody fusion with a porous nitinol implant. Global Spine J 2017;7:780–6.
[25] Zhou HZ, Hu M, Yao J, Ma L. Rapid lengthening of rabbit mandibular ramus by using nitinol spring: a preliminary study. J Craniofac Surg 2004;15:725–9.
[26] Shin DA, Yang BM, Tae G, Kim YH, Kim HS, Kim HI. Enhanced spinal fusion using a biodegradable porous mesh container in a rat posterolateral spinal fusion model. Spine J 2014;14:408–15.
[27] Brighton CT, Luessenhop CP, Pollack SR, Steinberg DR, Petrik ME, Kaplan FS. Treatment of castration-induced osteoporosis by a capacitively coupled electrical signal in rat vertebrae. J Bone Joint Surg Am Vol 1989;71:228–36.
[28] Ishida W, Elder BD, Holmes C, Lo SL, Witham TF. Variables affecting fusion rates in the rat posterolateral spinal fusion model with autogenic/allogenic bone grafts: a meta-analysis. Ann Biomed Eng 2016;44:3186–201.
[29] Yan M, Zhang C. Tilted plane Feldkamp type reconstruction algorithm for spiral cone beam CT. Med Phys 2005;32:3455–67.
[30] Lippman CR, Salehi SA, Liu JC, Ondra SL. Salvage technique of posterior iliac bolt placement in long-segment spinal constructs with a previous posterior iliac crest harvest: technical note. Neurosurgery 2006;58(1 Suppl). ONS-E178; discussion ONS-E.
[31] Gan JC, Glazer PA. Electrical stimulation therapies for spinal fusions: current concepts. Eur Spine J 2006;15:1301–11.
[32] Drespe IH, Polzhofer GK, Turner AS, Grauer JN. Animal models for spinal fusion. Spine J 2005;5(6 Suppl):209s–16s.
[33] Bostan B, Gunes T, Asci M, Sen C, Kelestemur MH, Erdem M, et al. Simvastatin improves spinal fusion in rats. Acta Orthopaedica et traumatologica turcica 2011;45:270–5.
[34] Kucharzyk DW. A controlled prospective outcome study of implantable electrical stimulation with spinal instrumentation in a high-risk spinal fusion population. Spine 1999;24:465–8. discussion 9.
[35] Tejano NA, Puno R, Ignacio JM. The use of implantable direct current stimulation in multilevel spinal fusion without instrumentation. A prospective clinical and radiographic evaluation with long-term follow-up. Spine 1996;21:1904–8.
[36] Mooney V. A randomized double-blind prospective study of the efficacy of pulsed electromagnetic fields for interbody lumbar fusions. Spine 1990;15:708–12.
[37] Steinmann JC, Herkowitz HN. Pseudarthrosis of the spine. Clin Orthop Relat Res 1992(284):80–90.
[38] Zdeblick TA. A prospective, randomized study of lumbar fusion. Preliminary results. Spine 1993;18:983–91.
[39] Dwyer AF. Use of direct current in spine fusion. J Bone Joint Surg 1974;56:442.
[40] Dejardin LM, Kahanovitz N, Arnoczky SP, Simon BJ. The effect of varied electrical current densities on lumbar spinal fusions in dogs. Spine J 2001;1:341–7.
[41] Bozic KJ, Glazer PA, Zurakowski D, Simon BJ, Lipson SJ, Hayes WC. In vivo evaluation of coralline hydroxyapatite and direct current electrical stimulation in lumbar spinal fusion. Spine 1999;24:2127–33.
[42] Kahanovitz N, Arnoczky SP. The efficacy of direct current electrical stimulation to enhance canine spinal fusions. Clin Orthop Relat Res 1990: 295–9.
[43] Nerubay J, Marganit B, Bubis JJ, Tadmor A, Katznelson A. Stimulation of bone formation by electrical current on spinal fusion. Spine 1986;11:167–9.
[44] Wright KC, Wallace S, Charnsangavej C, Carrasco CH, Gianturco C. Percutaneous endovascular stents: an experimental evaluation. Radiology 1985;156:69–72.
[45] Jung GS, Song HY, Seo TS, Park SJ, Koo JY, Huh JD, et al. Malignant gastric outlet obstructions: treatment by means of coaxial placement of uncovered and covered expandable nitinol stents. J Vasc Interv Radiol 2002;13:275–83.
[46] Odurny A. Colonic anastomotic stenoses and Memotherm stent fracture: a report of three cases. Cardiovasc Interv Radiol 2001;24:336–9.
[47] Yoon CJ, Song HY, Shin JH, Bae JI, Jung GS, Kichikawa K. et al. Malignant duodenal obstructions: palliative treatment using self-expandable nitinol stents. J Vasc Interv Radiol 2006;17:319–26.
[48] Goodwin CB, Brighton CT, Guyer RD, Johnson JR, Light KI, Yuan HA. A double-blind study of capacitively coupled electrical stimulation as an adjunct to lumbar spinal fusions. Spine 1999;24:1349–56. discussion 57.
[49] Linovitz RJ, Pathria M, Bernhardt M, Green D, Law MD, McGuire RA, et al. Combined magnetic fields accelerate and increase spine fusion: a double-blind, randomized, placebo controlled study. Spine 2002;27:1383–9. discussion 9.